Journal of Inflammation Research

Dovepress
Taylor & Francis Group

Open Access Full Text Article

ORIGINAL RESEARCH

Serum Pyroptosis-Related Cytokines as Biomarkers for Diagnostic Assessment and Risk Stratification of Ocular Graft-versus-Host Disease: A Case-Control Study

Jing Lou[1,2], Yue Xu[2], Xinyu Zhuang[2], Ye Zhao[1], Hui Pan[2], Yingjie Chen[2], Xiaofeng Zhang[2], Peirong Lu[1]

[1]Department of Ophthalmology, The First Affiliated Hospital of Soochow University, Suzhou, People's Republic of China; [2]Department of Ophthalmology, The Fourth Affiliated Hospital of Soochow University (Suzhou Dushu Lake Hospital), Suzhou, People's Republic of China

Correspondence: Xiaofeng Zhang, Department of Ophthalmology, The Fourth Affiliated Hospital of Soochow University (Suzhou Dushu Lake Hospital), Suzhou, Jiangsu Province, People's Republic of China, Email zhangxiaofeng@suda.edu.cn; Peirong Lu, Department of Ophthalmology, The First Affiliated Hospital of Soochow University, Suzhou, People's Republic of China, Email lupeirong@suda.edu.cn

Background: Ocular graft-versus-host disease (oGVHD) often presents with subtle and nonspecific symptoms following allogeneic hematopoietic stem cell transplantation (allo-HSCT). Current diagnostic methods primarily depend on subjective clinical evaluations with limited sensitivity. This study aimed to identify serum pyroptosis-related cytokines associated with oGVHD and to develop a cytokine-based diagnostic model.

Methods: In this prospective case–control study, 116 allo-HSCT recipients (61 with oGVHD and 55 without) and 47 healthy controls were enrolled. A sandwich antibody array was used to screen differentially expressed proteins in a pilot cohort (n = 4 per group), followed by pathway enrichment analysis. Ocular surface parameters and serum levels of NLRP3, TLR4, CCL2, IL-18, IL-6, and TNF-α were measured. Linear correlation, logistic regression, receiver operating characteristic (ROC) analyses, and internal bootstrap validation were performed to evaluate diagnostic performance. A cytokine-based risk score model was established.

Results: Thirty-four upregulated proteins were enriched in immune and inflammatory pathways. Patients with oGVHD exhibited severe dry eye features and significantly higher serum levels of NLRP3, TLR4, CCL2, IL-18, and IL-6 (all $p < 0.001$), which inversely correlated with ocular surface parameters. A logistic model combining these five cytokines achieved excellent diagnostic accuracy (AUC = 0.960). Internal 10-fold cross-validation with 1,000 bootstrap iterations yielded a consistent mean AUC of 0.953, confirming model robustness. A simplified risk score stratified patients into low-, intermediate-, and high-risk categories with strong discriminatory power ($p < 0.001$).

Conclusion: A serum panel of NLRP3, TLR4, CCL2, IL-18, and IL-6 demonstrates high diagnostic accuracy and stability for oGVHD. As the diagnostic cutoffs were derived from the same dataset, potential overfitting cannot be excluded, and independent validation in larger multicenter cohorts is warranted.

Keywords: ocular graft-versus-host disease, pyroptosis, cytokines, dry eye, case-control study

Introduction

Allogeneic hematopoietic stem cell transplantation (allo-HSCT) is a potentially curative therapy for a variety of hematologic malignancies and non-malignant disorders.[1,2] However, graft-versus-host disease (GVHD) remains one of its most serious complications, markedly affecting patients' quality of life.[3] Ocular graft-versus-host disease (oGVHD) is the most prevalent organ-specific manifestation of GVHD, with an incidence rate of up to 60%, and exceeding 90% in patients with concomitant systemic GVHD.[4] Clinically, oGVHD typically presents as severe dry eye disease, characterized by symptoms such as ocular dryness, foreign body sensation, burning, photophobia, and fluctuating vision.[5] These manifestations contribute to a substantial

Received: 18 July 2025
Accepted: 11 December 2025
Published: 19 December 2025

decline in vision-related quality of life. Studies have reported that oGVHD patients experience markedly reduced general health scores. Many individuals require the use of lubricating eye drops more than ten times per day, and in some cases, must limit outdoor activities due to vision impairment.[6,7] In addition to the severity of dry eye symptoms, oGVHD is often accompanied by extensive ocular surface dysfunction and notable psychological distress.[8,9]

Currently, the diagnosis of oGVHD primarily relies on clinical signs and subjective symptom assessments, such as the Ocular Surface Disease Index (OSDI), Schirmer I test, and corneal or conjunctival staining.[10–12] However, early-stage manifestations of oGVHD are often subtle and nonspecific, which makes them difficult to detect through routine clinical evaluations. Subjective assessments may be easily overlooked, and existing diagnostic tools exhibit limited sensitivity. Moreover, these methods are associated with inter-observer variability and lack objective serological indicators.[13,14] Consequently, some patients may experience delayed diagnosis, leading to progressive and irreversible damage to the ocular surface. Therefore, there is an urgent need for the development of objective and highly sensitive biomarkers to enable early detection and effective risk stratification of oGVHD.

In recent years, several potential biomarkers for oGVHD have been investigated, including tear cytokines such as IL-6, IL-8, and CXCL10, matrix metalloproteinases, and proteomic profiles derived from tear film analysis.[15–17] Although these studies have enhanced our understanding of ocular surface inflammation, the diagnostic applicability of tear-based biomarkers remains limited due to variability in sample collection, reflex tearing, and localized ocular surface alterations, which may not accurately represent systemic immune activity.[18] In contrast, serum biomarkers provide a more stable and accessible sample source and are less influenced by local ocular conditions, making them suitable for standardized diagnostic testing and large-scale screening.

Pyroptosis, a highly inflammatory form of programmed cell death, has recently been recognized as a key contributor to the pathogenesis of systemic GVHD. It is characterized by inflammasome activation and the subsequent release of proinflammatory cytokines such as IL-1β and IL-18, which amplify immune responses and exacerbate tissue injury.[19] Donor-derived macrophages and T cells can initiate pyroptotic cascades that promote Th1/Th17 polarization and accelerate GVHD progression.[20,21] Although the roles of Toll-like receptors (TLRs) and NOD-like receptors (NLRs) in GVHD have been explored,[22,23] their involvement in ocular GVHD remains poorly defined. Most oGVHD studies to date have primarily focused on T cell-mediated inflammation and fibrotic remodeling,[24] leaving the downstream pyroptotic pathways largely uncharacterized. However, previously described inflammatory pathways do not fully account for the marked cytokine surge and epithelial barrier disruption observed in oGVHD. Pyroptosis, by contrast, uniquely integrates innate immune activation with cytokine amplification and tissue injury, thereby representing a particularly relevant mechanism for elucidating the systemic–ocular inflammatory crosstalk. Notably, the TLR4–NOD-like receptor protein 3 (NLRP3)–IL-1β/IL-18 axis is known to sustain immune activation in various chronic inflammatory diseases, yet its role in oGVHD has not been systematically investigated.

Based on these findings, the present study employed a serum protein microarray to identify differentially expressed proteins associated with oGVHD, with a particular focus on pyroptosis-related inflammatory cytokines. The clinical relevance of these candidate markers was further evaluated, and a diagnostic scoring model incorporating key serum cytokines was developed. In this study, the proposed cytokine panel is intended for diagnostic assessment and risk stratification of oGVHD, providing preliminary, biologically plausible evidence for objective biomarkers and a practical framework to guide individualized patient management.

Patients and Methods

Patients

Study Population

This prospective study enrolled 116 patients who underwent allo-HSCT and were diagnosed at the Fourth Affiliated Hospital of Soochow University (Dushu Lake Hospital, Suzhou) between January 2022 and October 2024. Based on the presence or absence of oGVHD, patients were categorized into oGVHD and non-oGVHD groups. Additionally, 47 age- and sex-matched healthy volunteers were recruited as the normal control group.

Inclusion and Exclusion Criteria

Inclusion Criteria

1. Patients diagnosed by hematologists as having undergone allo-HSCT;
2. Age ≥ 15 years;
3. Classification into oGVHD or non-oGVHD groups based on the 2014 NIH chronic GVHD diagnostic criteria and the ICCGVHD consensus, with independent assessment of both ocular and systemic features;
4. Presence of dry eye signs in the anterior segment of both eyes; the eye with more severe involvement was selected for analysis. If both eyes were equally affected, the right eye was chosen by default;
5. No history of prior ocular treatment.

Exclusion Criteria

1. History of ocular conditions that could interfere with the diagnosis of oGVHD, such as previously diagnosed dry eye disease or corneal ulceration;
2. Presence of systemic autoimmune diseases (eg, systemic lupus erythematosus, ankylosing spondylitis) or ocular immune-mediated disorders (eg, cicatricial pemphigoid, Stevens–Johnson syndrome);
3. Ocular surgery performed within the preceding 3 months;
4. Inability to independently complete ophthalmic examinations or questionnaires due to poor general health status.

Methods

General Data Collection

Demographic and clinical information were recorded for all participants, including age, underlying hematologic disease prior to transplantation, time elapsed since allo-HSCT, HLA matching status, and relevant comorbidities.

Measurement of Best-Corrected Visual Acuity (BCVA) and Intraocular Pressure (IOP)

BCVA was assessed using a standard logarithmic visual acuity chart. IOP was measured using a non-contact tonometer; each eye was tested three times and the average value was recorded.

Detection of Differentially Expressed Proteins (DEPs)

A sandwich-based antibody microarray (AAH-BLG-TOL-4, RayBiotech, USA) was employed to measure the expression levels of 181 target proteins involved in Toll-like and NOD-like receptor signaling pathways. Serum samples were processed according to the manufacturer's instructions, including dialysis and sequential incubation with biotinylated detection reagents and Cy3-conjugated streptavidin. Fluorescent signals were detected using a microarray scanner (InnoScan 300, Innopsys, France) and analyzed using Q-Analyzer software (RayBiotech). The raw fluorescence intensities were $\log_2$-transformed for subsequent statistical analyses.

Corneal and Conjunctival Fluorescein Staining Scores

Fluorescein sodium strips were applied to the inferior conjunctival fornix, and patients were instructed to blink several times to evenly distribute the dye. Corneal and conjunctival staining were examined using a slit lamp microscope under cobalt blue light at 16× magnification. Corneal staining was graded according to the National Eye Institute (NEI) scoring system,[25] which divides the cornea into four quadrants and assigns a score ranging from 0 to 3 for each quadrant (total score range: 0–12). Conjunctival staining was assessed using the van Bijsterveld scoring system,[26] which evaluates staining in the nasal bulbar conjunctiva, temporal bulbar conjunctiva, and corneal region, with each area scored from 0 to 3. Only the conjunctival scores were included in the final analysis.

Ocular Surface Disease Index (OSDI)

The OSDI questionnaire consists of 12 items that evaluate ocular symptoms, visual function, and environmental triggers experienced over the preceding week. Each item is scored from 0 to 4. The total OSDI score was calculated using the

formula: OSDI = ([sum of scores] × 25) / [number of valid responses], yielding a maximum score of 100.[27] Investigators ensured that participants fully understood all questions before completing the questionnaire.

Schirmer I Test

The Schirmer I test was performed without topical anesthesia. Standardized Schirmer test strips were folded at the notch and placed at the junction between the lateral one-third and medial two-thirds of the lower conjunctival fornix. After 5 minutes with eyes closed, the strips were removed, and the length of wetting was measured and recorded in millimeters.

Noninvasive Ocular Surface Assessment

A corneal topography–based analyzer (Keratograph 5M, OCULUS, Germany) was used to assess ocular surface parameters. The mean noninvasive tear break-up time (NIBUT) was recorded to evaluate tear film stability. Tear volume was estimated by measuring the central inferior tear meniscus height (TMH). Meibomian gland dropout was graded on a scale of 0–3 (0 = no loss; 1 = ≤1/3 loss; 2 = >1/3 to ≤2/3 loss; 3 = >2/3 loss), with the combined upper and lower eyelid score range of 0–6. Bulbar conjunctival hyperemia was automatically quantified by the device's software and categorized as none (<0.10), mild (0.10–0.20), moderate (0.20–0.30), or severe (>0.30). All assessments were performed under standardized conditions of lighting and temperature. Subjects were instructed to blink naturally and fixate on a central target. Data acquisition and analysis were fully automated to minimize observer bias.

Tear Lactoferrin and Lysozyme C Measurement

As previously described by our team,[28],300 μL of sterile saline was instilled into the inferior conjunctival sac, and subjects were instructed to rotate their eyes to ensure complete mixing. Tear samples were collected from the inferior conjunctival fornix using capillary tubes, carefully avoiding direct contact with the ocular surface epithelium and without the use of topical anesthesia. Samples were then aliquoted into EP tubes and stored at −80°C. Lactoferrin and lysozyme C concentrations were measured using a double-antibody sandwich ELISA method.

Measurement of Serum Pyroptosis-Related Cytokines

Peripheral venous blood samples were collected from all participants, and serum was separated by centrifugation and stored at −80°C. Serum concentrations of key pyroptosis-associated cytokines, including NLRP3, TLR4, CCL2, IL-18, IL-6, TNF-α, CXCL2, STAT1, STAT2, JAK1, and AKT2, were quantified using enzyme-linked immunosorbent assays (ELISAs). The assay procedure involved precoating 96-well plates with specific capture antibodies, incubation with standards and serum samples, sequential addition of biotin-labeled detection antibodies and HRP-conjugated streptavidin, followed by colorimetric detection. Optical density was read at 450 nm, and cytokine concentrations were calculated based on standard curves.

The ELISA kits used in this study were as follows:NLRP3 (ab274401, Abcam, UK), TLR4 (EH460RB, Thermo Fisher Scientific, USA), CCL2 (DCP00, R&D Systems, USA), IL-18 (7620, MBL International, Japan), IL-6 (KHC0061, Thermo Fisher Scientific, USA), TNF-α (NBP1-91170, Novus Biologicals, USA), CXCL2 (OKCD07517, Aviva Systems Biology, USA), STAT1 (CBA034, Merck Millipore, USA), STAT2 (NBP3-40521, Novus Biologicals, USA), JAK1 (MBS2021168, MyBioSource, USA), and AKT2 (ab208986, Abcam, UK). All assays were performed in duplicate, and both intra- and inter-assay coefficients of variation were maintained below 10%.

Statistical Analysis

Statistical analyses were performed using SPSS version 27.0 (IBM Corp., Armonk, NY, USA), GraphPad Prism version 10.0 (GraphPad Software, San Diego, CA, USA), and R version 4.3.2 (R Foundation for Statistical Computing, Vienna, Austria). Proteomic microarray data were background-corrected, quantile-normalized, and $\log_2$-transformed prior to analysis. Differentially expressed proteins (DEPs) were identified using the limma package, with *p*-values adjusted for multiple testing by the Benjamini–Hochberg false discovery rate (FDR); FDR < 0.05 was considered statistically significant.

The sample size was initially determined based on prior studies and expected effect sizes to ensure adequate statistical power (≥80%) for detecting differences in serum cytokine levels between groups. Continuous variables were summarized as mean ± SD or median (IQR), and categorical variables as frequencies and percentages. Group comparisons were performed using the independent samples *t*-test or Mann–Whitney *U*-test for continuous variables, and the chi-square test for categorical variables. For comparisons across more than two groups, one-way ANOVA or Kruskal–Wallis *H*-test was applied. Spearman's rank correlation was used to evaluate associations between serum cytokine levels and ocular surface parameters.

Variables with $p < 0.10$ in univariate analyses were included in multivariate logistic regression models to identify independent predictors of oGVHD, adjusting for age, sex, time since allo-HSCT, and systemic cGVHD. A cytokine-based diagnostic score was developed using weighted regression coefficients, with continuous biomarker values to avoid dichotomization. Model performance was assessed by ROC analysis (*AUC*, sensitivity, specificity), and internal validation was performed using 10-fold cross-validation with 1,000 bootstrap iterations. Youden index–derived cutoffs were used for illustrative stratification. The calibration curve was evaluated through calibration curves constructed from cross-validated predictions to avoid overfitting bias. Post hoc power analysis confirmed adequate sample size (*power* >0.8). All tests were two-sided, with $p < 0.05$ or FDR < 0.05 considered statistically significant.

Results

Study Design and Workflow Overview

A preliminary proteomic screening was performed using a pyroptosis-related antibody array on serum samples obtained from 4 patients with oGVHD and 4 non-oGVHD controls. DEPs were identified and subsequently subjected to bioinformatic pathway enrichment analysis to explore their potential biological functions and associated signaling pathways. Key candidate biomarkers were subsequently selected for validation in an expanded clinical cohort. Correlation analyses were then performed between validated serum biomarkers and ocular surface parameters associated with dry eye severity. Finally, a predictive model incorporating the identified serum biomarkers was established to assess the feasibility of a blood-based diagnostic strategy for oGVHD. The overall study design and analytical workflow are illustrated in Figure 1.

Identification of DEPs

To identify potential serum biomarkers associated with oGVHD, we employed the AAH-BLG-TOL-4 protein array, which is designed to target key components of the Toll-like receptor and NOD-like receptor signaling pathways. Following normalization of the raw data, principal component analysis (PCA) revealed a clear separation between the oGVHD and non-oGVHD groups (Figure 2A), indicating distinct differences in their serum proteomic profiles. To control for false positives arising from multiple comparisons, the Benjamini–Hochberg false discovery rate (FDR)

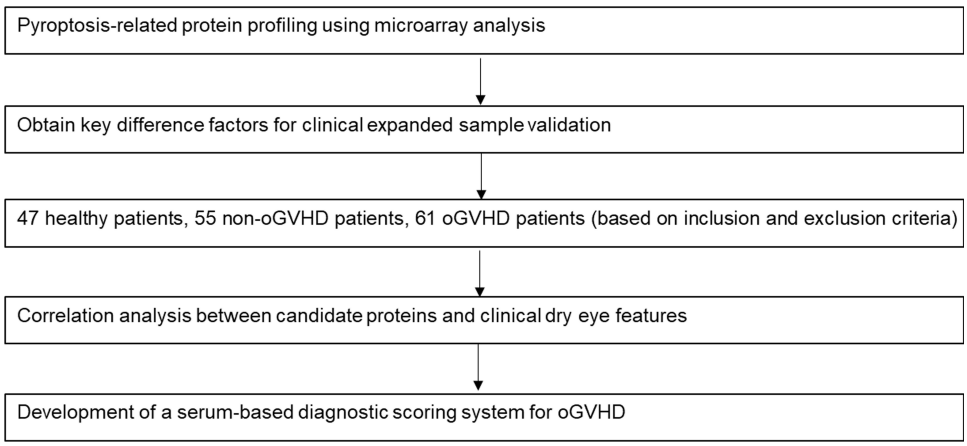

Figure 1 Schematic illustration of the overall study design and workflow.

https://doi.org/10.2147/JIR.S552170

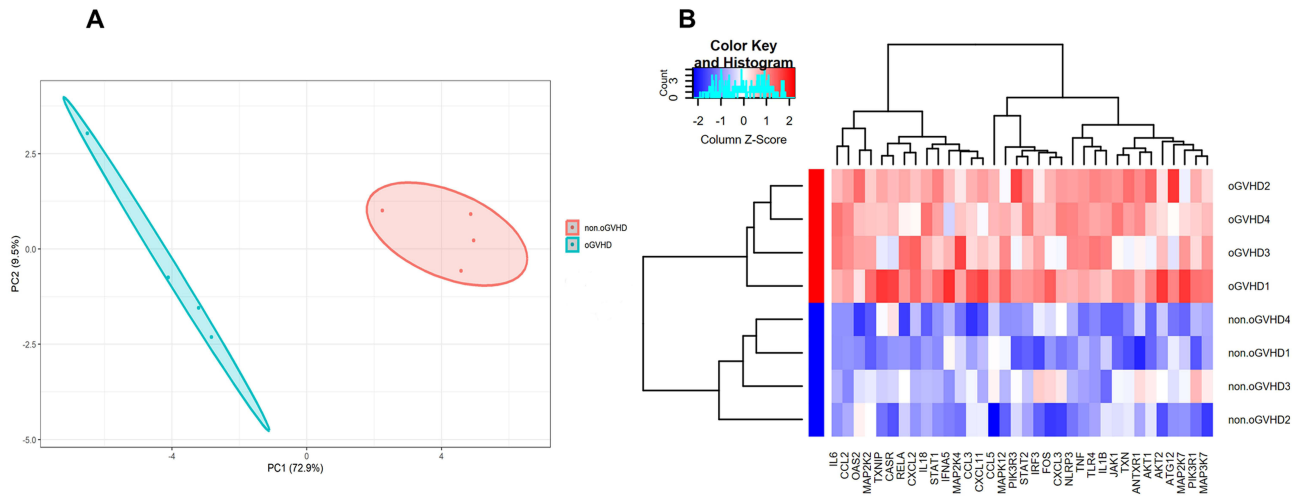

Figure 2 Principal component and hierarchical clustering analyses of differentially expressed proteins between oGVHD and non-oGVHD groups. **(A)** Principal component analysis (PCA) plot based on protein expression profiles from the AAH-BLG-TOL-4 array demonstrates clear separation between oGVHD (blue) and non-oGVHD (red) samples, indicating distinct proteomic patterns. **(B)** Heatmap with hierarchical clustering of 34 differentially expressed proteins (DEPs), all upregulated in the oGVHD group. Each column represents a sample, and each row corresponds to a specific protein. Expression levels are Z-score normalized; red indicates higher expression and blue indicates lower expression. Clustering distinguishes oGVHD from non-oGVHD samples based on expression signatures.

correction was applied, and proteins with adjusted p-values (FDR < 0.05) were considered significantly differentially expressed. Based on this criterion, a total of 34 DEPs were identified, all of which were significantly upregulated in the oGVHD group. Hierarchical clustering confirmed that these DEPs displayed distinct proteomic signatures, effectively distinguishing between the two clinical phenotypes (Figure 2B).

Gene Ontology (GO) and Kyoto Encyclopedia of Genes and Genomes (KEGG) Pathway Enrichment Analysis

To further elucidate the potential biological mechanisms involved in oGVHD, Gene Ontology (GO) and KEGG pathway enrichment analyses were performed on the 34 DEPs.The GO analysis revealed that the most significantly enriched biological processes (BP) were primarily associated with cellular response to biotic stimulus, response to lipopolysaccharide, and response to molecules of bacterial origin (Figure 3A). In terms of cellular components (CC), the enriched terms were predominantly related to the phosphatidylinositol 3-kinase complex and phagocytic cup structures (Figure 3B). For molecular functions (MF), the top enriched categories included cytokine receptor binding, cytokine activity, and chemokine receptor binding (Figure 3C).

KEGG pathway enrichment analysis demonstrated that DEPs were significantly overrepresented in several immune- and inflammation-related pathways, including the NOD-like receptor signaling pathway, the Toll-like receptor signaling pathway, and lipid metabolism and atherosclerosis (Figure 3D).

Baseline Characteristics of the Healthy Control, oGVHD, and Non-oGVHD Groups

In the oGVHD group, patients presented with various underlying hematologic malignancies, with acute myeloid leukemia (AML) being the most common diagnosis, accounting for 41.38% of cases. The mean interval from hematopoietic stem cell transplantation (HSCT) to the onset of ocular GVHD was 9.8 months, with a median of 10 months (range: 1–36 months).

As summarized in Table 1, no statistically significant differences were observed among the healthy control, non-oGVHD, and oGVHD groups in terms of age, sex distribution, or intraocular pressure (IOP) (all $p > 0.05$). However, compared to the other two groups, patients with oGVHD exhibited significantly worse best-corrected visual acuity (BCVA), higher corneal and conjunctival staining scores, and elevated Ocular Surface Disease Index (OSDI) scores (all $p < 0.001$), indicating more severe ocular surface involvement.

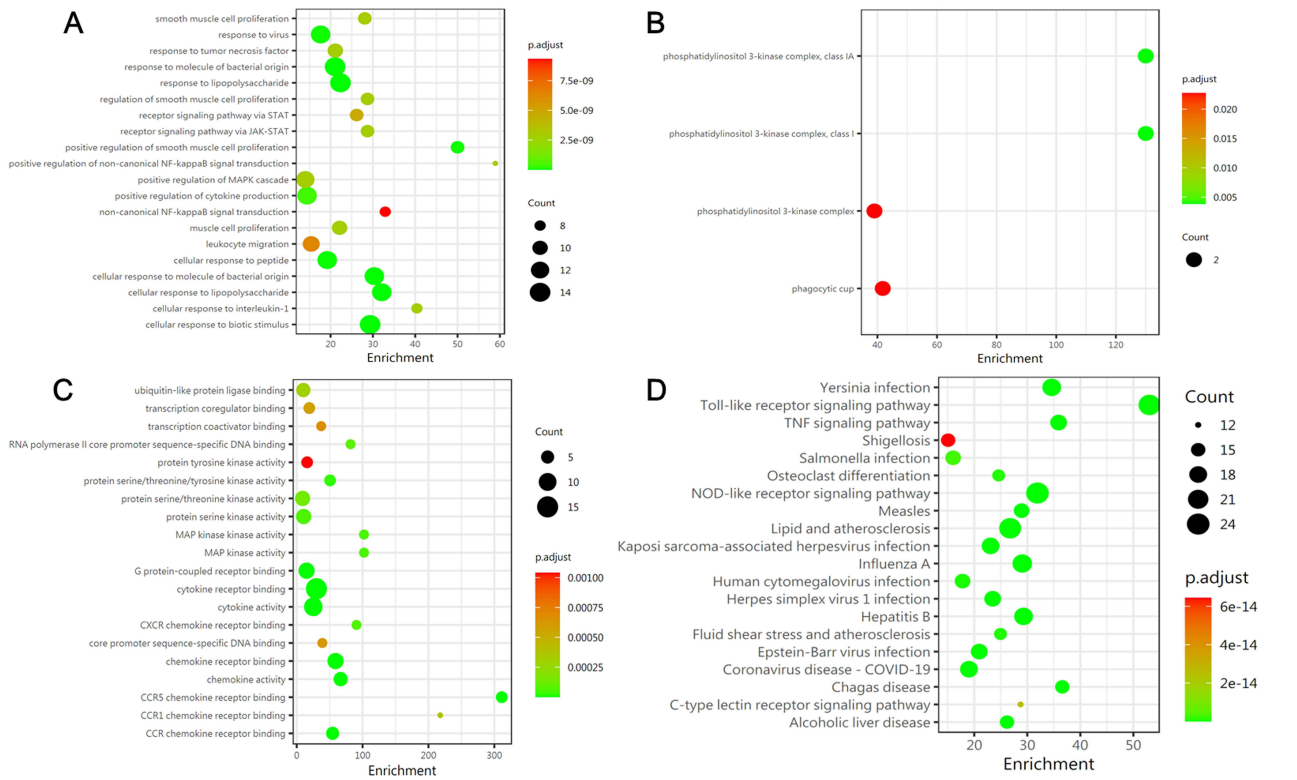

Figure 3 Bioinformatic analysis of differentially expressed proteins in oGVHD. (**A–C**) GO enrichment analysis of DEPs in the categories of Biological Process (BP), Cellular Component (CC), and Molecular Function (MF). (**D**) KEGG pathway analysis of DEPs. The size of each circle represents the number of proteins involved, and the color gradient reflects the adjusted p-value (p. adjust).

Comparison of Dry Eye Parameters and Tear Biomarkers Between oGVHD and Non-oGVHD Groups

A comparative analysis of dry eye related parameters and tear biomarkers between patients with and without oGVHD revealed statistically significant differences. As shown in Table 2, patients in the oGVHD group exhibited significantly shorter NIBUT, higher meibomian gland dropout scores, and increased conjunctival hyperemia compared to the non-oGVHD group. TMH, Schirmer I test scores, and the concentrations of tear lactoferrin and lysozyme were significantly lower in the oGVHD group (all $p < 0.001$), indicating more pronounced ocular surface damage and tear film instability in these patients.

Serum Levels of Key Pyroptosis Factors in Healthy Controls, Non-oGVHD, and oGVHD Patients

Based on the results from the protein microarray analysis, representative regulatory and effector molecules involved in the pyroptosis pathway were selected for further investigation. As shown in Table 3 and illustrated in Figure 4, ELISA

Table 1 Baseline Demographic and Clinical Characteristics of Healthy Controls, Non-oGVHD, and oGVHD Patients

Parameter	Healthy Control (n = 47)	Non-oGVHD (n = 55)	oGVHD (n = 61)	*p*-value
Age (years)	36.66 ± 11.79	35.29 ± 11.16	37.66 ± 12.21	0.557
Gender (male/female)	25/22	32/23	36/25	0.814
IOP (mmHg)	16.67 ± 2.02	16.55 ± 2.40	15.73 ± 3.04	0.108
BCVA (logMAR)	0.10 (0.00–0.10)	0.10 (0.00–0.10)	0.30 (0.10–0.52)	<0.001
Corneal staining score	1.00 (0.00–1.00)	1.00 (1.00–1.00)	9.00 (6.00–10.50)	<0.001
Conjunctival staining score	1.00 (0.00–1.00)	1.00 (1.00–1.00)	4.00 (3.00–5.00)	<0.001
OSDI score	11.01 ± 1.36	12.62 ± 2.24	45.99 ± 15.18	<0.001

https://doi.org/10.2147/JIR.S552170

Table 2 Comparison of Dry Eye Parameters and Tear Biomarkers Between oGVHD and Non-oGVHD Groups

Parameter	Non-oGVHD (n = 55)	oGVHD (n = 61)	*p*-value
NIBUT (s)	9.89 (5.93–13.70)	3.82 (0.03–5.30)	<0.001
TMH (mm)	0.25 ± 0.11	0.13 ± 0.05	<0.001
Meibomian gland dropout score	2.67 ± 1.30	4.17 ± 1.51	<0.001
Conjunctival hyperemia score	1.33 ± 0.55	2.67 ± 0.94	<0.001
Schirmer I test score (mm)	11.00 (10.00–13.00)	4.00 (2.00–5.50)	<0.001
Tear lactoferrin (mg/mL)	1.47 (1.25–1.65)	0.63 (0.33–0.98)	<0.001
Tear lysozyme (mg/mL)	1.67 (1.54–1.83)	0.59 (0.38–0.83)	<0.001

Table 3 Serum Protein Levels in Healthy Controls, Non-oGVHD, and oGVHD Groups

Serum Protein (Unit)	Healthy Control (n = 47)	Non-oGVHD Group (n = 55)	oGVHD Group (n = 61)	*p*-value
NLRP3 (ng/mL)	1.51 (1.14–1.89)	3.31 (2.70–4.23)	4.86 (4.10–6.21)	<0.001
TLR4 (ng/mL)	0.95 (0.72–1.28)	1.18 (0.89–1.79)	2.12 (1.69–3.07)	<0.001
CCL2 (pg/mL)	18.88 (10.16–21.52)	23.32 (19.64–27.88)	29.64 (27.12–37.66)	<0.001
IL-18 (pg/mL)	186.75 (174.50–215.25)	215.00 (192.25–244.25)	381.38 (285.82–428.82)	<0.001
IL-6 (pg/mL)	3.42 (2.30–4.39)	4.78 (3.57–5.70)	7.56 (5.29–8.93)	<0.001
TNF-α (pg/mL)	3.87 (2.74–5.36)	5.67 (4.14–7.59)	8.00 (5.04–10.13)	<0.001
CXCL2 (ng/mL)	4.28 (3.16–5.28)	4.34 (2.98–5.77)	4.85 (3.90–6.00)	0.170
STAT1 (pg/mL)	0.61 (0.54–0.72)	0.62 (0.52–0.71)	0.66 (0.57–0.76)	0.194
STAT2 (pg/mL)	6.46 (5.44–7.72)	7.11 (5.64–7.97)	6.88 (5.81–7.72)	0.434
JAK1 (pg/mL)	0.29 (0.22–0.48)	0.30 (0.21–0.45)	0.32 (0.24–0.52)	0.548
AKT2 (pg/mL)	0.13 (0.08–0.16)	0.10 (0.05–0.17)	0.14 (0.06–0.20)	0.246

results revealed that serum levels of NLRP3, TLR4, IL-18, CCL2, IL-6, and TNF-α were significantly elevated in the oGVHD group compared to both the non-oGVHD and healthy control groups (all $p < 0.001$). In contrast, no statistically significant differences were observed in the serum concentrations of the remaining five pyroptosis-related factors among the three groups (all $p > 0.05$). A post hoc power analysis based on the observed effect sizes indicated that the study had adequate statistical power (>0.8) to detect the observed group differences in key cytokines.

Correlation Between Dry Eye Parameters and Key Pyroptosis-Related Factors

To investigate the association between inflammatory markers and ocular surface damage, correlation analyses were performed between key pyroptosis-related serum factors and dry eye parameters in both oGVHD and non-oGVHD groups. As shown in Table 4, the expression levels of NLRP3, TLR4, CCL2, IL-18, IL-6, and TNF-α exhibited significant negative correlations with multiple clinical indicators of dry eye severity.

Specifically, higher levels of these inflammatory markers were associated with shorter noninvasive tear break-up time (NIBUT), reduced tear meniscus height (TMH), lower Schirmer I test values, and decreased concentrations of lactoferrin and lysozyme (all $p < 0.05$). Notably, IL-18 showed the strongest correlations with both Schirmer I test values ($r = -0.587$, $p < 0.01$) and lysozyme levels ($r = -0.587$, $p < 0.01$). These findings highlight the strong link between pyroptosis-related inflammation and tear film instability as well as lacrimal gland dysfunction in patients with oGVHD.

Logistic Regression Analysis of Key Factors

Binary logistic regression analysis was conducted to assess the association between the occurrence of oGVHD and six pyroptosis-related serum biomarkers listed in Table 4, including NLRP3, TLR4, CCL2, IL-18, IL-6, and TNF-α. The primary aim was to construct a diagnostic model capable of distinguishing patients with oGVHD from those without.

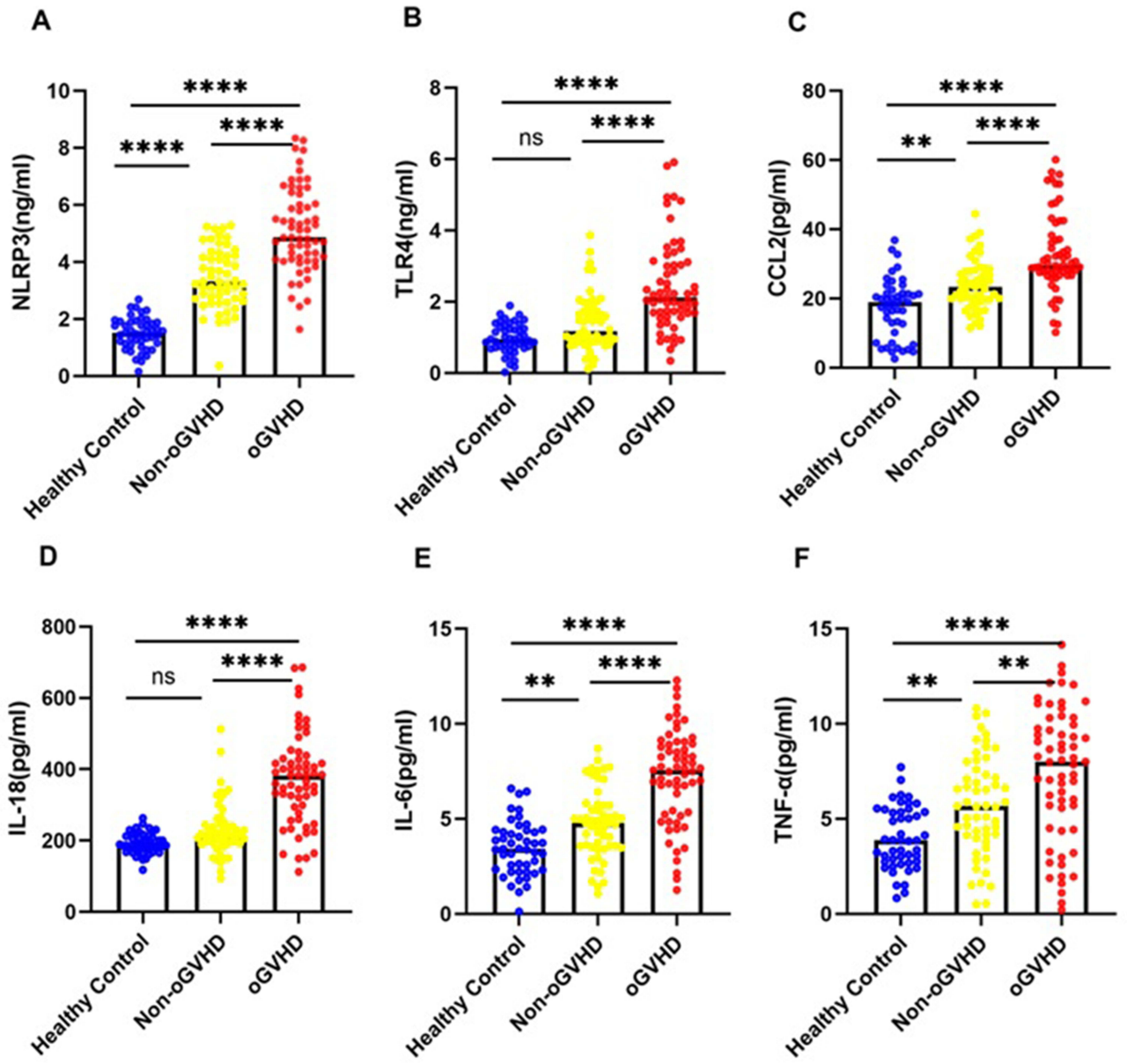

Figure 4 Differential serum levels of key pyroptosis-related cytokines among healthy controls, non-oGVHD patients, and oGVHD patients. **(A)** Serum NLRP3 levels. **(B)** Serum TLR4 levels. **(C)** Serum CCL2 levels. **(D)** Serum IL-18 levels. **(E)** Serum IL-6 levels. **(F)** Serum TNF-α levels. Data are presented as mean ± standard deviation (SD). Comparisons among the three groups were performed using one-way analysis of variance (ANOVA) followed by Tukey's post hoc test for normally distributed data, or Kruskal–Wallis *H*-test followed by Dunn's post hoc test for non-normally distributed data, as appropriate. Significant levels; $^{**}p < 0.01$; $^{****}p < 0.0001$. $p < 0.05$ was considered statistically significant.
Abbreviation: ns, not significant.

As shown in Table 5, all six variables exhibited odds ratios (ORs) greater than 1.0, suggesting potential positive associations with oGVHD. Among them, NLRP3, TLR4, CCL2, IL-18, and IL-6 showed statistically significant associations ($p < 0.05$), suggesting their potential as independent diagnostic markers. Although TNF-α also demonstrated an elevated OR (1.268; 95% CI: 0.999–1.609), the association did not reach statistical significance ($p = 0.051$). After adjusting for potential confounders, including age, sex, time post-transplant, and systemic cGVHD, NLRP3, TLR4, CCL2, IL-18, and IL-6 remained significantly associated with oGVHD (all adjusted $p < 0.05$), indicating their independent diagnostic value.

https://doi.org/10.2147/JIR.S552170

Table 4 Correlations (r) Between Dry Eye Parameters and Pyroptosis-Related Cytokines in oGVHD and Non-oGVHD Patients

Factor	NIBUT (s)	TMH (mm)	Schirmer I (mm)	Lactoferrin (mg/mL)	Lysozyme (mg/mL)
NLRP3	-0.381**	-0.279**	-0.492**	-0.462**	-0.469**
TLR4	-0.262**	-0.333**	-0.368**	-0.411**	-0.448**
CCL2	-0.234*	-0.215*	-0.394**	-0.301**	-0.429**
IL-18	-0.416**	-0.383**	-0.587**	-0.436**	-0.587**
IL-6	-0.382**	-0.262**	-0.456**	-0.383**	-0.432**
TNF-α	-0.228*	-0.138	-0.279**	-0.108	-0.299**

Notes: Values are Spearman's correlation coefficients (r). *$p < 0.05$, **$p < 0.01$.

Table 5 Logistic Regression Analysis of Key Factors Associated with oGVHD (Based on Table 4)

Parameter	OR (95% CI)	*p*-value
NLRP3	3.065 (1.397–6.725)	0.005
TLR4	3.020 (1.148–7.944)	0.025
CCL2	1.123 (1.031–1.223)	0.008
IL-18	1.013 (1.005–1.021)	0.002
IL-6	1.616 (1.176–2.220)	0.003
TNF-α	1.268 (0.999–1.609)	0.051

Development of a Novel Risk Scoring System

To enhance diagnostic accuracy, a novel risk scoring system was established based on key pyroptosis-related serum biomarkers. The optimal diagnostic cut-off values for each biomarker were determined using the Youden index derived from receiver operating characteristic (ROC) curve analyses. These Youden-derived thresholds were used as exploratory indicators for model construction rather than fixed clinical cutoffs, acknowledging their potential dataset dependence. The expression levels of these biomarkers were then dichotomized into binary variables (0 or 1), depending on whether they were below or above their respective threshold values, as summarized in Table 6. These dichotomized indicators were subsequently incorporated into a binary logistic regression model to estimate their corresponding odds ratios (ORs), as shown in Table 7.

Logistic regression analysis revealed that all included biomarkers were significantly associated with oGVHD, with ORs ranging from 9 to 18 (all $p < 0.05$). The ORs were rounded to the nearest integers and assigned as weights to formulate the scoring algorithm. This newly established scoring system provides a semi-quantitative approach for estimating the probability of oGVHD, which may contribute to diagnostic assessment and support evidence-based clinical decision-making.

Diagnostic Performance of Inflammatory Biomarkers

Receiver operating characteristic (ROC) curve analyses were performed to evaluate the diagnostic performance of individual inflammatory biomarkers in predicting the occurrence of oGVHD. The area under the ROC curve (AUC)

Table 6 Construction of the Novel Scoring System Based on Optimal Cut-off Values

Parameter	Optimal Cut-off Value	Score	Optimal Cut-off Value	Score
NLRP3	≥3.99	1	<3.99	0
TLR4	≥1.67	1	<1.67	0
CCL2	≥25.84	1	<25.84	0
IL-18	≥320.31	1	<320.31	0
IL-6	≥6.57	1	<6.57	0

Table 7 Logistic Regression Analysis and OR Values for Scoring System Development

Parameter	OR (95% CI)	*p*-value
NLRP3	8.635 (1.649–45.216)	0.011
TLR4	11.535 (2.186–60.860)	0.004
CCL2	14.467 (2.850–73.438)	0.001
IL-18	18.069 (3.390–96.308)	0.001
IL-6	13.980 (2.971–65.786)	0.001

values were as follows: NLRP3 (AUC = 0.822; 95% CI: 0.747–0.897), TLR4 (AUC = 0.775; 95% CI: 0.690–0.860), CCL2 (AUC = 0.763; 95% CI: 0.674–0.853), IL-18 (AUC = 0.838; 95% CI: 0.762–0.915), and IL-6 (AUC = 0.783; 95% CI: 0.699–0.867). Among the individual biomarkers, IL-18 demonstrated the highest predictive accuracy.

As illustrated in Figure 5, a multivariate model incorporating all five biomarkers yielded significantly improved diagnostic performance, achieving an AUC of 0.960 (95% CI: 0.925–0.995), suggesting excellent discriminatory capability. All AUC values were significant compared to the reference line ($p < 0.001$, DeLong's test). These results highlight the potential clinical applicability of the combined biomarker panel for the noninvasive diagnosis of oGVHD.

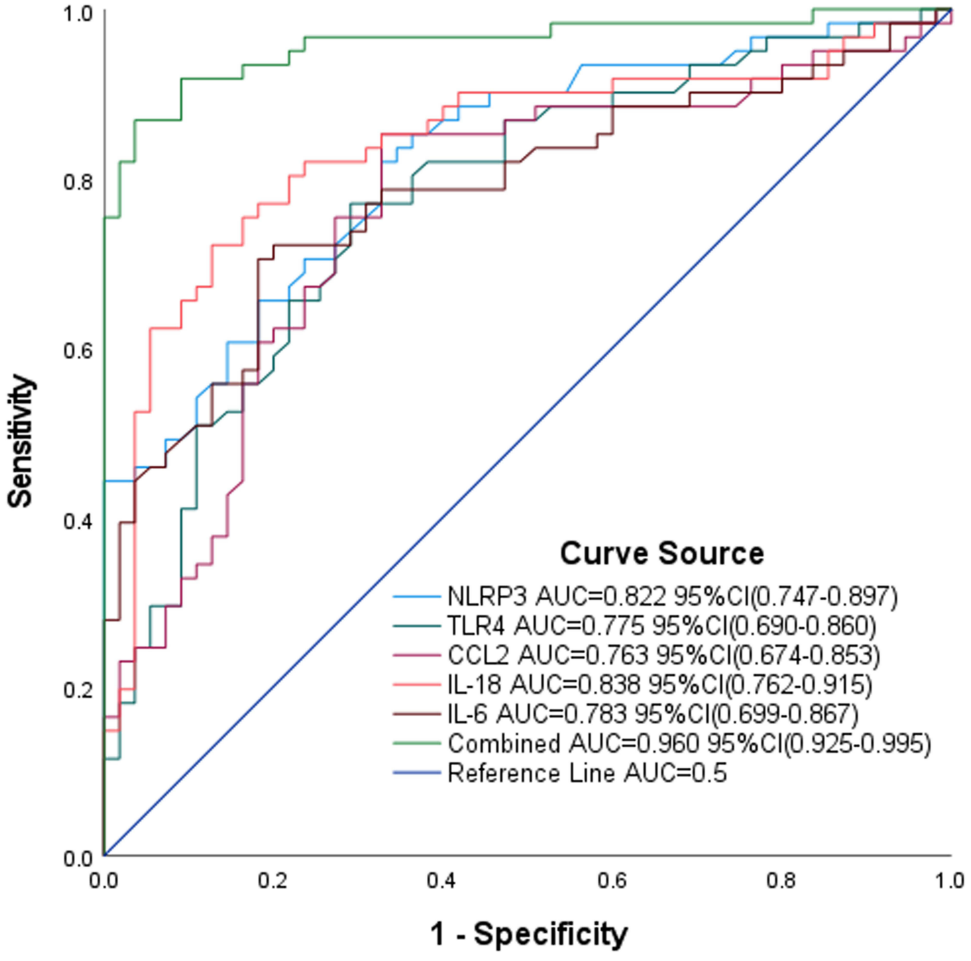

Figure 5 Receiver operating characteristic (ROC) curves depicting the diagnostic performance of individual inflammatory biomarkers (NLRP3, TLR4, CCL2, IL-18, and IL-6) and their combination for predicting oGVHD. The multivariate model achieved the highest diagnostic accuracy, with an area under the curve (AUC) of 0.953. The diagonal line represents the reference (non-informative) classifier with an AUC of 0.5.

https://doi.org/10.2147/JIR.S552170

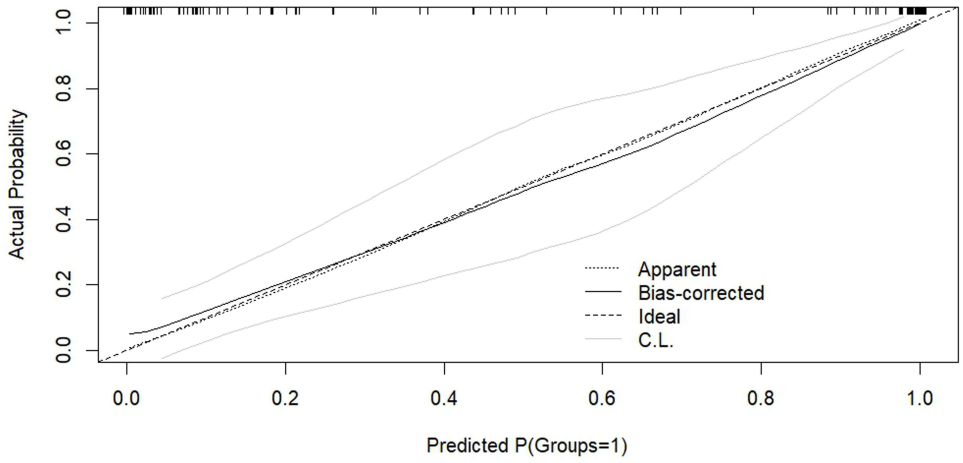

Figure 6 Calibration curve of the oGVHD diagnostic model. The calibration curve depicts the relationship between the predicted probabilities and observed frequencies of oGVHD. The bias-corrected calibration (solid line) was generated using bootstrap resampling with 1,000 iterations. The gray shaded area represents the 95% confidence interval of the bias-corrected curve. The dashed diagonal line indicates perfect calibration.

To minimize potential overfitting and assess the robustness of the diagnostic model, internal validation was conducted using 10-fold cross-validation combined with bootstrap resampling (1,000 iterations) within the discovery cohort. After bias correction through 1,000 bootstrap resampling iterations, the optimism-adjusted AUC was 0.953 (95% CI: 0.934–0.960), indicating minimal overfitting. The narrow confidence interval confirms robust performance across resampling scenarios. In addition, a calibration curve was also plotted for internal validation. The results demonstrated good agreement between predicted probabilities and observed outcomes across the full range of predictions (Figure 6). The bias-corrected calibration line closely approximated the ideal diagonal line, indicating excellent model stability and generalizability. These results further confirm the reliability of the combined biomarker panel for discriminating oGVHD from non-oGVHD patients.

Discriminative Ability of the Risk Scoring System

Based on the individual scores, the newly developed scoring system stratified patients into three risk categories: low risk (0–33 points), intermediate risk (34–50 points), and high risk (51–67 points). As shown in Table 8, among patients diagnosed with oGVHD, 5 (8.2%) were classified as low risk, 20 (32.8%) as intermediate risk, and 36 (59.0%) as high risk. In contrast, in the non-oGVHD group, 50 patients (90.9%) were classified as low risk, 5 (9.1%) as intermediate risk, and no patients fell into the high risk. The distribution of risk categories differed significantly between the oGVHD and non-oGVHD groups ($p < 0.001$), indicating that the scoring system possessed strong discriminatory capability in identifying patients with oGVHD. To evaluate the potential clinical net benefit of applying our diagnostic model in practice, we performed a decision curve analysis (DCA). This analysis quantifies the standardized net benefit of using the model across a spectrum of threshold probabilities—the minimum risk at which a clinician would consider initiating intervention. As depicted in Figure 7, the DCA demonstrated that the combined five-biomarker model (red curve) yielded a consistently higher net benefit than the strategies of "all" or "none" over a wide and clinically relevant range of threshold probabilities, approximately from 10% to 60%. This indicated that clinical decisions guided by our model would lead to superior patient outcomes by correctly identifying individuals who would benefit from intervention, while avoiding unnecessary procedures for those at low risk.

Table 8 Risk Stratification of Patients with and without oGVHD Based on the Newly Developed Scoring System

Risk Category	oGVHD (n = 61)	Non-oGVHD (n = 55)	*p*-value
Low Risk (0–33)	5 (8.2%)	50 (90.9%)	<0.001
Intermediate (34–50)	20 (32.8%)	5 (9.1%)	
High Risk (51–67)	36 (59.0%)	0 (0%)	

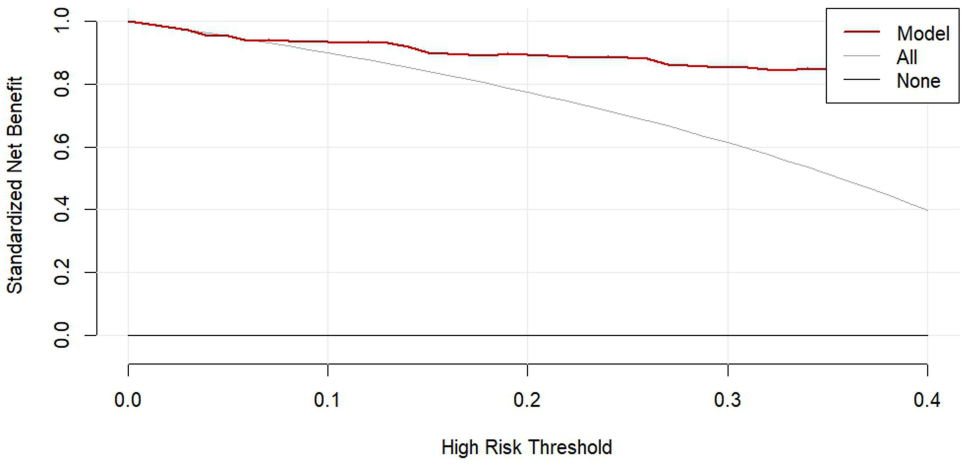

Figure 7 Decision curve analysis for the oGVHD diagnostic model. The net benefit is shown for three clinical strategies: using the diagnostic model to guide decision-making (red solid line), assuming all patients have oGVHD and require further intervention (gray solid line), and assuming no patient has oGVHD (black solid line). The model demonstrated superior clinical utility, as its net benefit curve remained above both comparator strategies across threshold probabilities ranging from 0.10 to 0.40.

Discussion

This study represents the first systematic demonstration of the critical role of pyroptosis in the pathogenesis of oGVHD following allo-HSCT. We observed significantly elevated serum levels of NLRP3, TLR4, CCL2, IL-18, and IL-6 in oGVHD patients compared to those without oGVHD, as well as healthy controls. These cytokines showed strong correlations with clinical dry eye parameters and exhibited high diagnostic accuracy within a multivariate predictive model. Rather than suggesting a definitive diagnostic utility, these findings primarily highlight the biological plausibility and pathway-level relevance of pyroptosis-related cytokines in the systemic immune dysregulation underlying oGVHD (Figure 8). Based on these findings, we developed a novel scoring system capable of stratifying patient risk levels, highlighting its potential value for diagnostic assessment and clinical management of oGVHD.

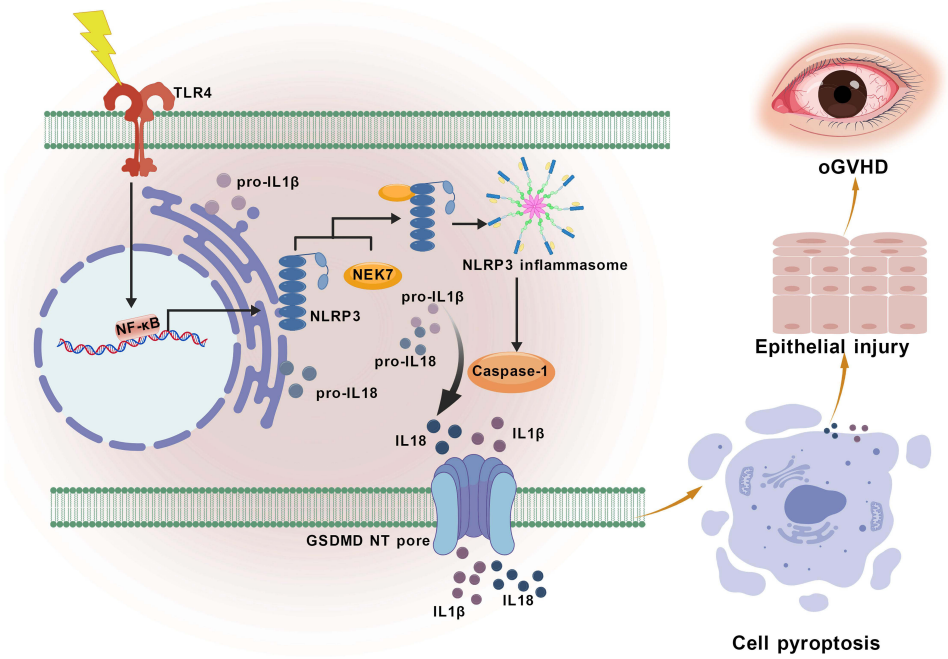

Figure 8 Pyroptosis-mediated ocular surface injury in oGVHD. Schematic of the TLR4/NLRP3/Caspase-1 signaling pathway in oGVHD. TLR4 activation primes NF-κB, upregulating NLRP3 and pro-IL-1β. A secondary signal triggers NLRP3 inflammasome assembly and Caspase-1 activation. Caspase-1 cleaves pro-IL-1β to mature IL-1β and gasdermin D (GSDMD) to GSDMD-NT, which forms membrane pores, releasing IL-1β and inflammatory mediators. This cascade induces epithelial pyroptosis and sustained inflammation, contributing to ocular surface damage in oGVHD.

https://doi.org/10.2147/JIR.S552170

Pyroptosis is an inflammatory form of programmed cell death that has been associated with the development of various autoimmune disorders and systemic GVHD.[29–31] In this study, we observed significantly elevated serum levels of NLRP3, TLR4, and their downstream effector cytokines—IL-18, IL-6, and CCL2—in patients with oGVHD. These findings suggest that pyroptosis driven by inflammasome activation, along with the subsequent cytokine cascade, may play a pivotal role in the pathophysiology of ocular surface damage in oGVHD.

Based on the dynamic expression of these biomarkers and their association with clinical phenotypes, we propose a three-stage pathogenic cascade involved in the development of oGVHD. In the initiation phase, elevated NLRP3 expression may promote pyroptosis through gasdermin D-mediated membrane pore formation, a mechanism previously reported in corneal epithelial cells under hyperosmotic stress and in environmental dry eye models.[32] Simultaneous upregulation of TLR4 suggests enhanced innate immune sensing and inflammasome activation.[33,34] Notably, the TLR4/NLRP3 signaling axis has also been associated with other chronic inflammatory disorders, such as Alzheimer's disease, where it contributes to neuroinflammation and disease progression.[35]

During the immune polarization phase, persistent elevation of IL-18 and IL-6 may drive Th1 and Th17 differentiation,[36,37] respectively, thereby contributing to the establishment of a chronic proinflammatory microenvironment. Importantly, IL-18 demonstrated the highest diagnostic accuracy in our study (AUC = 0.838), which aligns with its established role in mediating corneal epithelial apoptosis and impairing barrier function.[38] In the tissue damage phase, upregulation of chemokines such as CCL2 may facilitate monocyte recruitment to the ocular surface, resulting in epithelial injury. This mechanism is supported by studies in dry eye disease populations, where CCL2-mediated monocyte migration has been associated with inflammation-induced epithelial damage.[39]

Although TNF-α is a well-established cytokine in systemic GVHD,[40,41] its association with ocular involvement did not reach statistical significance in our study ($p = 0.051$). This finding aligns with recent reports suggesting that TNF-α lacks specificity in the pathophysiology of dry eye,[42,43] thereby reinforcing the hypothesis that oGVHD is governed by a distinct immunopathological mechanism.

We also found significant negative correlations between pyroptosis-related biomarkers and tear film stability parameters, including NIBUT and TMH, which reinforces the notion that inflammasome activation plays a role in ocular surface dysfunction, possibly through direct cytotoxic effects or by augmenting local immune responses.[44]

Currently, the diagnosis of oGVHD primarily relies on subjective clinical symptoms and physical signs, which are often insufficiently sensitive for detecting the disease at early stage. In this context, the biomarker panel proposed in our study offers an objective and minimally invasive alternative for diagnosis, demonstrating potential utility in identifying patients who are asymptomatic or exhibit atypical manifestations. The multivariate model incorporating NLRP3, TLR4, IL-18, IL-6, and CCL2 achieved an area under the curve (AUC) of 0.960, markedly surpassing the diagnostic performance of any single biomarker. Furthermore, based on internal validation using 1,000 bootstrap resamples, the calibration curve demonstrated that bias-corrected calibration line closely approximated the ideal diagonal line, confirming the robustness and reliability of the model's discriminative performance.

The scoring system we developed facilitates practical clinical application by stratifying patients into low-, intermediate-, and high-risk groups. Notably, 59% of oGVHD patients were classified as high-risk, compared to 0% in the non-oGVHD group, highlighting the model's ability to effectively differentiate between these patient populations. These findings support that serum pyroptosis-associated cytokines may serve as objective and minimally invasive biomarkers, contributing to the early identification of oGVHD. This risk stratification approach has the potential to inform personalized treatment strategies, enabling the timely initiation of immunomodulatory therapy in high-risk patients to mitigate ocular surface damage.

The compelling diagnostic accuracy of our five-biomarker panel underscores its potential as an objective tool for oGVHD assessment. However, high discrimination accuracy alone does not guarantee clinical usefulness. To evaluate whether using this model in practice would improve patient outcomes, we performed a DCA. Within the critical decision threshold range of 0.10–0.40, the model achieved a maximum net benefit of 0.12. For a patient whose model-predicted probability falls above a clinician's threshold for action, the DCA shows that acting on this prediction—by initiating a comprehensive ophthalmological workup or preemptive immunomodulatory therapy—provides a net positive outcome. This facilitates early intervention in high-risk individuals before irreversible ocular surface damage occurs. Conversely, for patients below this threshold, the model reliably identifies a low-risk group in whom intervention can be safely

deferred, thus avoiding unnecessary treatment and optimizing resource allocation. This approach moves beyond subjective symptom assessment towards a risk-based, personalized management paradigm. However, it is crucial to emphasize that the proposed cut-off values and model are derived from this initial case-control cohort. Therefore, a critical next step is the validation of these biomarkers and the refinement of the scoring system in large, prospective, multicenter studies before they can be routinely integrated into clinical decision-making algorithms.

However, several limitations must be acknowledged. First, the discovery phase was based on a small exploratory cohort (n = 4 per group), and the findings should therefore be interpreted with caution until confirmed in larger, independent populations. In addition, variability in the underlying hematologic disorders and post-transplant treatment regimens among allo-HSCT recipients may have contributed to inter-individual differences, along with potential confounding influences from systemic GVHD activity, concurrent infections, or ongoing immunosuppressive therapy. Second, the diagnostic model has yet to undergo independent external validation, and its generalizability remains to be determined. The Youden index–based thresholds were derived from the same dataset and should be regarded as preliminary, pending confirmation in future multicenter investigations. Inter-assay variability between different commercial platforms or laboratory-developed tests could affect the absolute concentration values obtained. Therefore, the translation of our proposed cut-off values to other clinical settings would require careful calibration and standardization to ensure consistent performance and interpretability across different laboratories. Moreover, the cross-sectional nature of the study precludes inference of temporal or causal relationships between cytokine alterations and oGVHD onset, underscoring the need for prospective longitudinal studies. The single-center design may also limit the broader applicability of the results. Finally, the mechanistic connections between serum cytokine alterations and local ocular immune microenvironment changes (eg, in the cornea and conjunctiva) remain incompletely understood. While this study focused on serum biomarkers as a stable and accessible sample source, we did not perform a parallel analysis of tear cytokine levels. Future studies integrating tear proteomics, impression cytology, ocular surface biopsies, in vivo confocal microscopy, and tissue cytokine analysis will be crucial to further elucidate the pathogenic mechanisms underlying oGVHD.

Conclusion

This study provides preliminary evidence that pyroptosis-related cytokines may serve as serum biomarkers for oGVHD and highlights their potential pathological relevance. A panel comprising NLRP3, TLR4, CCL2, IL-18, and IL-6 demonstrated good diagnostic performance in the current cohort, and a risk score–based stratification offers a practical approach for clinical risk assessment. Nonetheless, the findings are limited by the case-control design, small sample size, and potential confounding factors such as time since transplantation and concomitant treatments, which may lead to optimistic performance estimates. Accordingly, these results should be interpreted cautiously, and further validation in larger, prospective, multicenter studies is warranted to confirm their diagnostic utility and assess their clinical applicability.

Abbreviations

AKT2, AKT serine/threonine kinase 2; allo-HSCT, allogeneic hematopoietic stem cell transplantation; AML, acute myeloid leukemia; ANOVA, analysis of variance; AUC, area under the curve; BCVA, best-corrected visual acuity; BP, biological processes; CC, cellular components; CCL2, C-C motif chemokine ligand 2; CI, confidence interval; CXCL2, C-X-C motif chemokine ligand 2; DEPs, differentially expressed proteins; ELISA, enzyme-linked immunosorbent assay; GO, Gene Ontology; GVHD, graft-versus-host disease; HSCT, hematopoietic stem cell transplantation; ICCGVHD, International Chronic Ocular Graft-versus-Host Disease; IL-18, Interleukin-18; IL-6, Interleukin-6; IOP, intraocular pressure; IQR, interquartile range; JAK1, Janus kinase 1; KEGG, Kyoto Encyclopedia of Genes and Genomes; logMAR, logarithm of the minimum angle of resolution; MF, molecular functions; NEI, National Eye Institute; NIBUT, noninvasive tear break-up time; NIH, National Institutes of Health; NLRP3, NOD-like receptor protein 3; NLRs, NOD-like receptors; oGVHD, ocular graft-versus-host disease; OR, odds ratio; OSDI, Ocular Surface Disease Index; PCA, principal component analysis; ROC, receiver operating characteristic; SD, standard deviation; STAT1, signal transducer and activator of transcription 1; STAT2, signal transducer and activator of transcription 2; Th1, T helper 1; Th17, T helper 17; TLR4, Toll-like receptor 4; TLRs, Toll-like receptors; TMH, tear meniscus height; TNF-α, tumor necrosis factor-alpha.

Data Sharing Statement

All data supporting the findings of this study are included within the article.

Ethics Approval and Informed Consent

This study was conducted in accordance with the Declaration of Helsinki and was approved by the Ethics Committee of the Fourth Affiliated Hospital of Soochow University (Suzhou Dushu Lake Hospital) (Approval No. 220001). Written informed consent was obtained from all participants after a full explanation of the study objectives and procedures. Informed consent for underage participants was obtained from their parents or legal guardians.

Acknowledgments

The authors would like to express their sincere gratitude to the clinical staff at the Department of Ophthalmology, the Fourth Affiliated Hospital of Soochow University (Suzhou Dushu Lake Hospital), and the First Affiliated Hospital of Soochow University for their valuable assistance with patient recruitment and clinical coordination. The authors also thank all the patients and healthy volunteers who generously participated in this study.

Funding

This work was supported by the Suzhou Clinical Key Diseases Diagnosis and Treatment Technology Special Project (LCZX202236).

Disclosure

The authors declare that they have no competing interests.

References

1. Shahzad M, Amin MK, Khalid MF, et al. Outcomes with allogeneic hematopoietic stem cell transplantation in therapy related myeloid neoplasms: a systematic review and meta-analysis. *Clin Lymphoma Myeloma Leuk*. 2025;25(5):e319–e335. doi:10.1016/j.clml.2024.12.018
2. Mahmoud HK, Elhaddad AM, Fahmy OA, et al. Allogeneic hematopoietic stem cell transplantation for non-malignant hematological disorders. *J Adv Res*. 2015;6(3):449–458. doi:10.1016/j.jare.2014.11.001
3. Blazar BR, Murphy WJ, Abedi M. Advances in graft-versus-host disease biology and therapy. *Nat Rev Immunol*. 2012;12(6):443–458. doi:10.1038/nri3212
4. Giannaccare G, Bonifazi F, Sessa M, et al. Ocular surface analysis in hematological patients before and after allogeneic hematopoietic stem cell transplantation: implication for daily clinical practice. *Eye*. 2017;31(10):1417–1426. doi:10.1038/eye.2017.78
5. Wolff D, Radojcic V, Lafyatis R, et al. National institutes of health consensus development project on criteria for clinical trials in chronic graft-versus-host disease: IV. The 2020 highly morbid forms report. *Transplant Cell Ther*. 2021;27(10):817–835. doi:10.1016/j.jtct.2021.06.001
6. Saboo US, Amparo F, Abud TB, Schaumberg DA, Dana R. Vision-related quality of life in patients with ocular graft-versus-host disease. *Ophthalmology*. 2015;122(8):1669–1674. doi:10.1016/j.ophtha.2015.04.011
7. Baral P, Kumaran S, Stapleton F, Pesudovs K. A systematic review assessing the quality of patient reported outcome measures in ocular surface disease. *Ocul Surf*. 2025;35:31–56. doi:10.1016/j.jtos.2024.11.011
8. Jacobs JM, Fishman S, Sommer R, et al. Coping and modifiable psychosocial factors are associated with mood and quality of life in patients with chronic graft-versus-host disease. *Biol Blood Marrow Transplant*. 2019;25(11):2234–2242. doi:10.1016/j.bbmt.2019.06.024
9. El-Jawahri A, Pidala J, Khera N, et al. Impact of psychological distress on quality of life, functional status, and survival in patients with chronic graft-versus-host disease. *Biol Blood Marrow Transplant*. 2018;24(11):2285–2292. doi:10.1016/j.bbmt.2018.07.020
10. Jagasia MH, Greinix HT, Arora M, et al. National institutes of health consensus development project on criteria for clinical trials in chronic graft-versus-host disease: i. the 2014 diagnosis and staging working group report. *Biol Blood Marrow Transplant*. 2015;21(3):389–401.e1. doi:10.1016/j.bbmt.2014.12.001
11. Rapoport Y, Freeman T, Koyama T, et al. Validation of International chronic ocular graft-versus-host disease (GVHD) group diagnostic criteria as a chronic ocular GVHD-specific metric. *Cornea*. 2017;36(2):258–263. doi:10.1097/ico.0000000000001109
12. Ogawa Y, Kim SK, Dana R, et al. International chronic ocular graft-vs-host-disease (GVHD) consensus group: proposed diagnostic criteria for chronic GVHD (Part I). *Sci Rep*. 2013;3(1):3419. doi:10.1038/srep03419
13. Na KS, Yoo YS, Hwang KY, Mok JW, Joo CK. Tear osmolarity and ocular surface parameters as diagnostic markers of ocular graft-versus-host disease. *Am J Ophthalmol*. 2015;160(1):143–9.e1. doi:10.1016/j.ajo.2015.04.002
14. Tappeiner C, Heiligenhaus A, Halter JP, Miserocchi E, Bandello F, Goldblum D. Challenges and concepts in the diagnosis and management of ocular graft-versus-host disease. *Front Med Lausanne*. 2023;10:1133381. doi:10.3389/fmed.2023.1133381
15. Bohlen J, Gomez C, Zhou J, Martinez Guasch F, Wandvik C, Sunshine SB. Molecular biomarkers in ocular graft-versus-host disease: a systematic review. *Biomolecules*. 2024;14(1):102. doi:10.3390/biom14010102
16. Soleimani M, Mahdavi Sharif P, Cheraqpour K, et al. Ocular graft-versus-host disease (oGVHD): from A to Z. *Surv Ophthalmol*. 2023;68(4):697–712. doi:10.1016/j.survophthal.2023.02.006

17. Pietraszkiewicz AA, Payne D, Abraham M, et al. Ocular surface indicators and biomarkers in chronic ocular graft-versus-host disease: a prospective cohort study. *Bone Marrow Transplant*. 2021;56(8):1850–1858. doi:10.1038/s41409-021-01254-5
18. Cheng X, Huang R, Huang S, et al. Recent advances in ocular graft-versus-host disease. *Front Immunol*. 2023;14:1092108. doi:10.3389/fimmu.2023.1092108
19. Lu Y, Meng R, Wang X, et al. Caspase-11 signaling enhances graft-versus-host disease. *Nat Commun*. 2019;10(1):4044. doi:10.1038/s41467-019-11895-2
20. Sun X, Qu Q, Chen Q, et al. Donor macrophage pyroptosis contributes to the development of aGVHD. *Sci China Life Sci*. 2025;68(9):2605–2616. doi:10.1007/s11427-024-2908-8
21. Chen W, Su G, Xu Y, et al. Caspase-1 inhibition ameliorates murine acute graft versus host disease by modulating the Th1/Th17/Treg balance. *Int Immunopharmacol*. 2021;94:107503. doi:10.1016/j.intimp.2021.107503
22. Toubai T, Mathewson ND, Magenau J, Reddy P. Danger signals and graft-versus-host disease: current understanding and future perspectives. *Front Immunol*. 2016;7:539. doi:10.3389/fimmu.2016.00539
23. Nogai A, Heimesaat MM, Thiele M, et al. Toll-like receptors 2 and 4 are involved in the induction of graft-versus-host-disease in mice. *Blood*. 2006;108(11):5175. doi:10.1182/blood.V108.11.5175.5175
24. Ogawa Y, Kawakami Y, Tsubota K. Cascade of inflammatory, fibrotic processes, and stress-induced senescence in chronic GVHD-related dry eye disease. *Int J Mol Sci*. 2021;22(11):6114. doi:10.3390/ijms22116114
25. Lemp MA. Report of the national eye institute/industry workshop on clinical trials in dry eyes. *Clao J*. 1995;21(4):221–232.
26. Herbaut A, Liang H, Rabut G, et al. Impact of dry eye disease on vision quality: an optical quality analysis system study. *Transl Vis Sci Technol*. 2018;7(4):5. doi:10.1167/tvst.7.4.5
27. Schiffman RM, Christianson MD, Jacobsen G, Hirsch JD, Reis BL. Reliability and validity of the ocular surface disease index. *Arch Ophthalmol*. 2000;118(5):615–621. doi:10.1001/archopht.118.5.615
28. Chen Y, Zhuang X, Wang L, et al. The role of IL-6, IL-10, and TNF-α in ocular GVHD following allogeneic transplantation. *Ocul Immunol Inflamm*. 2024;32(8):1788–1795. doi:10.1080/09273948.2024.2302445
29. Jankovic D, Ganesan J, Bscheider M, et al. The Nlrp3 inflammasome regulates acute graft-versus-host disease. *J Exp Med*. 2013;210 (10):1899–1910. doi:10.1084/jem.20130084
30. Chen KW, Demarco B, Broz P. Beyond inflammasomes: emerging function of gasdermins during apoptosis and NETosis. *EMBO J*. 2020;39(2): e103397. doi:10.15252/embj.2019103397
31. Vasudevan SO, Behl B, Rathinam VA. Pyroptosis-induced inflammation and tissue damage. *Semin Immunol*. 2023;69:101781. doi:10.1016/j.smim.2023.101781
32. Zheng Q, Ren Y, Reinach PS, et al. Reactive oxygen species activated NLRP3 inflammasomes initiate inflammation in hyperosmolarity stressed human corneal epithelial cells and environment-induced dry eye patients. *Exp Eye Res*. 2015;134:133–140. doi:10.1016/j.exer.2015.02.013
33. Zhou R, Yazdi AS, Menu P, Tschopp J. A role for mitochondria in NLRP3 inflammasome activation. *Nature*. 2011;469(7329):221–225. doi:10.1038/nature09663
34. Guo H, Callaway JB, Ting JP. Inflammasomes: mechanism of action, role in disease, and therapeutics. *Nat Med*. 2015;21(7):677–687. doi:10.1038/nm.3893
35. Zhu M, Liu Y, Chen C, et al. TLR4/Rac1/NLRP3 pathway mediates amyloid-β-induced neuroinflammation in Alzheimer's disease. *J Alzheimers Dis*. 2024;99(3):911–925. doi:10.3233/jad-240012
36. Landy E, Carol H, Ring A, Canna S. Biological and clinical roles of IL-18 in inflammatory diseases. *Nat Rev Rheumatol*. 2024;20(1):33–47. doi:10.1038/s41584-023-01053-w
37. Ihim SA, Abubakar SD, Zian Z, et al. Interleukin-18 cytokine in immunity, inflammation, and autoimmunity: biological role in induction, regulation, and treatment. *Front Immunol*. 2022;13:919973. doi:10.3389/fimmu.2022.919973
38. Burbach GJ, Naik SM, Harten JB, et al. Interleukin-18 expression and modulation in human corneal epithelial cells. *Curr Eye Res*. 2001;23 (1):64–68. doi:10.1076/ceyr.23.1.64.5425
39. Nicolle P, Liang H, Reboussin E, et al. Proinflammatory markers, chemokines, and enkephalin in patients suffering from dry eye disease. *Int J Mol Sci*. 2018;19(4):1221. doi:10.3390/ijms19041221
40. Hu B, Qiu Y, Hong J. Tear cytokine levels in the diagnosis and severity assessment of ocular chronic graft-versus-host disease(GVHD). *Ocul Surf*. 2020;18(2):298–304. doi:10.1016/j.jtos.2019.12.005
41. Riemens A, Stoyanova E, Rothova A, Kuiper J. Cytokines in tear fluid of patients with ocular graft-versus-host disease after allogeneic stem cell transplantation. *Mol Vis*. 2012;18:797–802.
42. Ji YW, Byun YJ, Choi W, et al. Neutralization of ocular surface TNF-α reduces ocular surface and lacrimal gland inflammation induced by in vivo dry eye. *Invest Ophthalmol Vis Sci*. 2013;54(12):7557–7566. doi:10.1167/iovs.12-11515
43. Zhou Y, Murrough J, Yu Y, et al. Association between depression and severity of dry eye symptoms, signs, and inflammatory markers in the dream study. *JAMA Ophthalmol*. 2022;140(4):392–399. doi:10.1001/jamaophthalmol.2022.0140
44. Shamloo K, Mistry P, Barbarino A, Ross C, Jhanji V, Sharma A. Differential effect of proinflammatory cytokines on corneal and conjunctival epithelial cell mucins and glycocalyx. *Transl Vis Sci Technol*. 2021;10(7):17. doi:10.1167/tvst.10.7.17